SME Annual Meeting
Feb. 24 - 27, 2018, Denver, CO

Preprint 19-109

CONSIDERATIONS FOR BLAST SURVIVABILITY OF BUILT-IN-PLACE REFUGE ALTERNATIVE DOORS

D. S. Yantek, CDC NIOSH, Pittsburgh, PA
J. P. Homer, CDC NIOSH, Pittsburgh, PA
C. C. Jobes, CDC NIOSH, Pittsburgh, PA

ABSTRACT

In 2008, the Mine Safety and Health Administration (MSHA) mandated refuge alternatives (RAs) in underground coal mines. For RAs, federal regulations specify a design pressure of 103.4 kPa (15 psi). This paper discusses the blast response of built-in-place RA doors. Researchers at the National Institute for Occupational Safety and Health (NIOSH) performed linear static finite element (FE) analyses on a built-in-place (BIP) RA door using two loading conditions: a 103.4-kPa (15-psi) design pressure and a 20.7-kPa (3-psi) negative pressure. Both of the FE analyses showed that the door yielded. The information presented in this paper can be used to ensure that BIP RA stoppings and doors can withstand survivable explosions.

INTRODUCTION

Since 2008, the Mine Safety and Health Administration (MSHA) has required the installation of refuge alternatives (RAs) in underground coal mines [1]. RAs can provide trapped miners with a breathable air environment if miners cannot escape a mine after a mine accident, such as a fire or an explosion. In underground coal mines, from 1970 until the present, 15 explosions that killed more than five miners in each incident have occurred. In total, these mine disasters have killed 201 miners [2]. A review of underground coal mine disasters from 1970 through 2006 was conducted in order to assess the potential of RAs to save lives [3]. To examine the potential impact of RA use in underground coal mines, an event tree analysis was performed on 38 accidents, including 17 that killed more than five miners and 20 that killed from 1 to 4 miners. According to the analysis, RAs could have saved 74 of 252 miners who were killed, including 57 of 67 miners who died while trying to escape and 17 to 19 miners from two disasters that involved the use of barricades.

One of the incidents involving the use of barricades occurred in 2006 [4]. An explosion at Sago mine was responsible for killing 13 miners. One miner died from carbon monoxide shortly after the explosion, while the other 12 miners survived. In an attempt to establish a breathable atmosphere, the miners who survived the explosion constructed a barricade. Tragically, 11 of the 12 barricaded miners died from carbon monoxide poisoning.

Because explosions are the most common disaster in underground coal mines, it is critical for RAs to be able to withstand a survivable explosion. Military sources contain significant information on the ability of humans to survive explosions. Zipf and Cashdollar [5] examined multiple sources to investigate the effects of blast loading on the human body [6, 7, 8]. Overpressures of 241.3 to 310.3 kPa (35 to 45 psi) may cause only 1% fatalities, while overpressures of 379.2 to 448.2 kPa (55 to 65 psi) may cause 99% fatalities [6, 8].

Although humans can withstand significant overpressure without experiencing trauma, in the case of a blast, injuries caused by flying debris or by a person being driven into a hard object are responsible for most deaths [5]. Table 1 summarizes the effects of increasing blast pressure on various structures and the human body. As the table shows, most people would be killed at an overpressure of 68.9 kPa (10 psi), and fatalities approach 100% at 137.9 kPa (20 psi). In order to ensure RAs can be operated after a survivable explosion, RAs must withstand a design overpressure of 103.4 kPa (15 psi) for 0.2 sec [1]. This design pressure is further clarified to have a 0.1-second rise time [9].

In the case of built-in-place (BIP) RAs, both the stoppings and doors must withstand the design overpressure. Prior to the updated requirements for mine seals, numerous 137.9-kPa (20-psi) mine seal designs that could be used to construct a BIP RA were tested to withstand a 137.9-kPa (20-psi) overpressure [10]. These 137.9-kPa (20-psi) mine seal designs could serve as stoppings for BIP RAs. In *RI 9698 Facilitating the Use of Built-in-place Refuge Alternatives in Mine,* NIOSH proposed a design criteria for BIP RA stoppings and provided one example of applying these criteria to a BIP RA stopping [11]. The proposed NIOSH design criteria uses the same design overpressure of 103.4 kPa (15 psi) for 0.2 sec mandated by federal RA regulations and specifies the same elasticity of design requirement as federal mine seal regulations in 30 CFR 75.335 [1].

Table 1. The effects of various long duration blast overpressures and the associated maximum wind speeds on various structures and the human body [5].

Peak Over-pressure	Max. Wind Speed	Effect on Structures	Effect on the Human Body
6.9 kPa (1 psi)	61 kph (38 mph)	Window glass shatters.	Light injuries from fragments occur.
13.8 kPa (2 psi)	113 kph (70 mph)	Moderate damage to houses occurs (windows & doors blown out, severe roof damage).	People are injured by flying glass and debris.
20.7 kPa (3 psi)	164 kph (102 mph)	Residential structures collapse.	Serious injuries are common, fatalities may occur.
34.5 kPa (5 psi)	262 kph (163 mph)	Most bldgs collapse.	Injuries are universal, fatalities are widespread.
68.9 kPa (10 psi)	473 kph (294 mph)	Reinforced concrete bldgs are severely damaged or demolished.	Most people are killed.
137.9 kPa (20 psi)	807 kph (502 mph)	Heavily built concrete bldgs are severely damaged or demolished.	Fatalities approach 100%.

Although numerous mine seal designs that could serve as BIP RA stoppings have been demonstrated to withstand greater than the 103.4-kPa (15-psi) design pressure, the blast response of BIP RA doors has not been measured or analyzed. The door is a critical component of a BIP RA that must function after being subjected to a survivable explosion. This paper will discuss general blast response and a simplified analysis of a BIP RA door using a linear static finite element (FE) model.

BLAST RESPONSE

Determining the mechanical response of a structure to a blast requires knowledge of both the applied blast load and the structure's dynamic characteristics. In general, the response of a structure to a

dynamic load with a specified amplitude will not be the same as the response of the structure to a static load of the same amplitude. The discussion that follows provides details on structural dynamic response and blast load characteristics.

The simplest model that can be used to analyze the dynamic response of a system is called a single degree-of-freedom (SDOF) model. An SDOF model consists of a mass, a spring, and a damper with an applied force as shown in Figure 1. The mass is represented as *m*, the viscous damping coefficient is denoted as *c*, the spring rate is represented as *k*, the applied force is denoted as *F*, and the displacement of the mass is *z*.

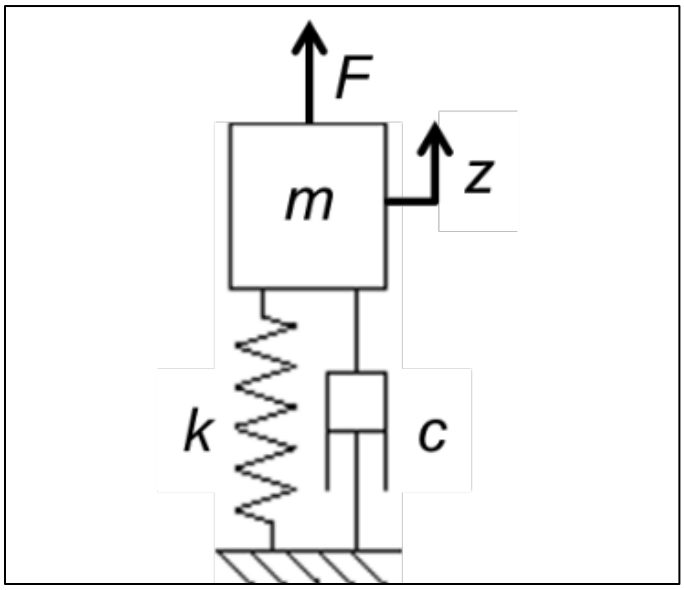

Figure 1. A single degree-of-freedom (SDOF) model.

In order to determine the response of the SDOF system, the equation of motion must be derived. For the SDOF system depicted in Figure 1, the equation of motion is:

$$m\ddot{z} + c\dot{z} + kz = F \tag{1}$$

where $\ddot{z}$ is the acceleration of the mass and $\dot{z}$ is the velocity of the mass. Equation 1 can be solved using numerical integration and other methods as described in *Biggs* [12]. To apply an SDOF model to a BIPRA door, an equivalent dynamic mass and bending stiffness can be estimated using the methods from Chapter 5 of *Biggs* [12].

In order to simplify the analysis of an SDOF system subjected to an impulsive force, such as a blast, *Biggs* defines a term called the dynamic load factor (DLF). The DLF is the ratio of the dynamic response to the dynamic load divided by the static response that would occur due to applying a static load with the same magnitude as the dynamic load. In equation form, the DLF is:

$$DLF = \frac{z}{z_{st}} \tag{2}$$

where z_{st} is the static deflection due to a static load *F* which is found by:

$$z_{st} = \frac{F}{k} \tag{3}$$

The maximum DLF is a function of the ratio of the impulse duration divided by the natural period of the structure. For a system with light damping, such as a BIPRA metal door, the effect of damping on the period of the structure can be ignored and the period is calculated by:

$$T = 2\pi\sqrt{\frac{m}{k}} \tag{4}$$

where *T* is the natural period of the door, *m* is the effective mass of the door, and *k* is the effective stiffness of the door.

The significance of the maximum DLF is that it allows the maximum dynamic response of a structure to be estimated using the results of a static analysis. Closed-form and empirical solutions for many simple beam- and plate-like structures can be found in the literature [13, 14]. Therefore, the maximum deflection and stress due to a dynamic load can be found by using the maximum DLF to scale the values found through static analysis.

In addition to being a function of the ratio of the impulse duration to the structure's period, the maximum DLF is also a function of the shape of the applied load. For an isosceles-triangle-shaped load, such as the 103.4-kPa (15-psi) design pressure, the maximum DLF has a peak value of about 1.5 when the ratio of t_d/T is about 0.88 as shown in Figure 2. When the ratio of the impulse duration to the natural period of the structure exceeds 4, the shape of the curve in Figure 2 suggests the maximum DLF is less than 1. The maximum DLFs for rectangular- and right-triangle-shaped loads are shown in Figure 3. For a rectangular-shaped load, the maximum DLF is 2 when the ratio of t_d/T exceeds 0.5. For a right-triangle-shaped load, the maximum DLF asymptotically approaches 2 as the ratio of t_d/T reaches 10.

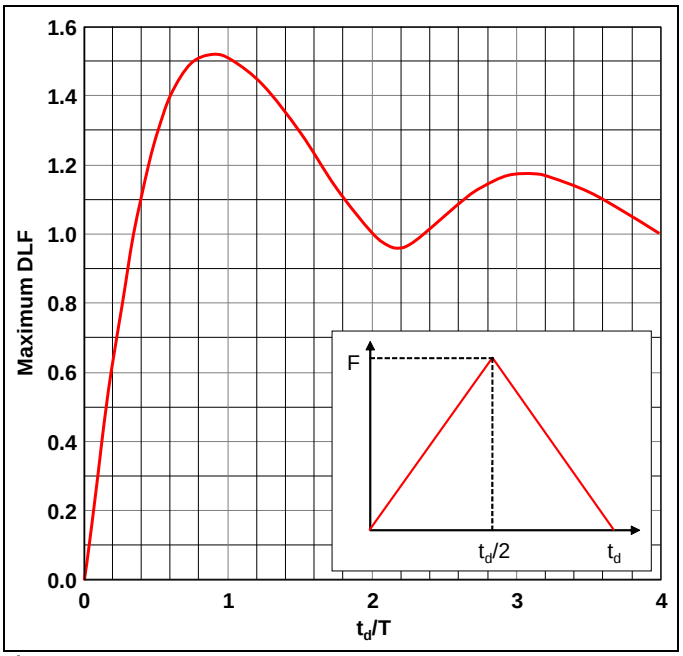

Figure 2. Maximum DLF for isosceles-triangle-shaped impulse loads from Biggs [12].

Although the maximum DLF can be utilized for simple, ideal loads and structures, real loads and structures can present some challenges because real loads do not generally have the exact form of a triangle or square, and, usually, closed-form solutions do not exist for real structures. In addition, real loads from blasts often have a negative component where the applied pressure dips below atmospheric pressure and a vacuum load is applied to the structure. Figure 4 shows pressure traces in A-drift at Lake Lynn Laboratory at various distances from the ignition source for explosion test #420. This test was conducted as part of NIOSH research on rapid mine seal design [15]. As the blast pressure propagates away from the source, several locations show a positive pressure of about 137.9 to 172.4 kPa (20 to 25 psi) with a subsequent negative pressure of about 20.7 to 34.5 kPa (3 to 5 psi).

For blast loads with a positive and negative component applied to a BIPRA door, the positive pressure would cause an inward deflection of the door and, assuming yielding or failure does not occur, the internal strain would force the door to rebound toward its original position, most likely with multiple oscillations. The negative pressure would tend to pull the door outward. Depending on the dynamic characteristics of the door, the negative pressure could add to the internal strain energy acting to force the door out. For an outswing door, the positive pressure applied to the door would be supported by

the door jamb, and the negative pressure and rebound load would be carried by the hinges and latching mechanisms only.

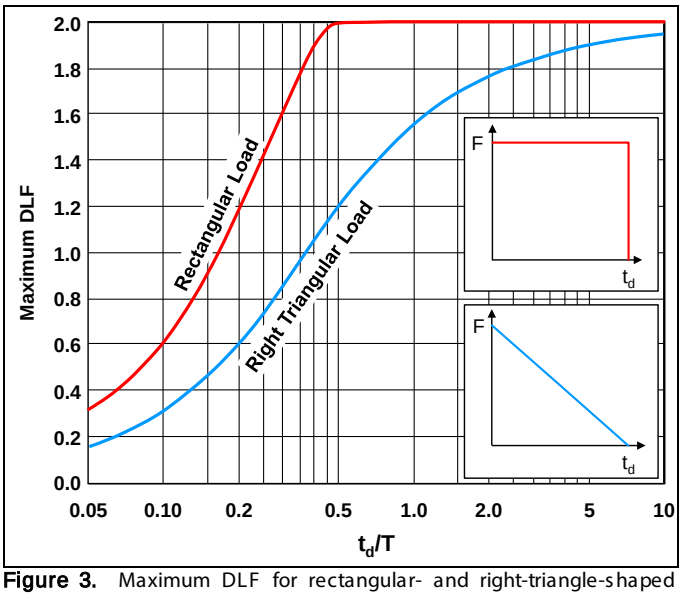

Figure 3. Maximum DLF for rectangular- and right-triangle-shaped impulse loads from Biggs [12].

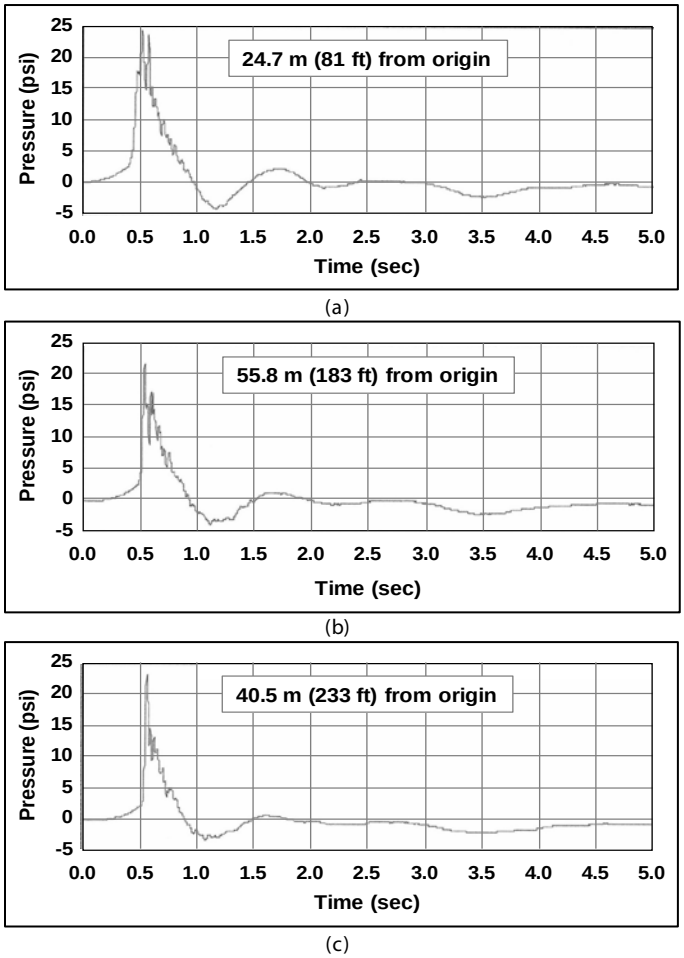

Figure 4. Blast loads measured at A-drift in Lake Lynn Laboratory at distances of (a) 24.7 m (81 ft), (b) 55.8 m (183 ft), and (c) 40.5 (233 ft) from the ignition point.

BIP RA DOOR FINITE ELEMENT ANALYSIS

In order to determine the maximum deflection and stresses on the door, hinges, and latching mechanisms, a linear static FE analysis was performed on the door. Because a BIP RA door should be designed so that yielding does not occur, a linear static FE analysis is appropriate for a first-cut analysis. It is important to note that a linear static model cannot predict stresses accurately if the stress exceeds the yield strength of the material because the model does not account for the non-linear material behavior that occurs due to yielding.

BIP RA Door

The subject of the analysis is the steel BIP RA door shown in Figure 5. The door is built using identical inner and outer door leaves attached to a support frame. The support frame is designed to be installed into a 0.41-m (16-inch) thick concrete block wall. The skin of the 0.91-m (36-inch) wide by 1.30-m (51-inch) tall door leaf has a thickness of 2.54 mm (0.1) inches. The door skin has an outward x-shaped raised profile that is intended to increase its bending stiffness. A 25.4-mm (1-inch) wide by 50.8 mm (2-inch) high by 1.52-mm (0.060-inch) thick rectangular tube is attached to the inside of the door skin to act as a stiffener (see Figure 5b). The door uses a single door latch with a 19.1-mm (0.75-inch) diameter latch pin and a 6.35-mm (0.25-inch) thick latch plate (see Figure 5c), and two hinges with 1.59-mm (0.63-inch) diameter hinge pins (see Figure 5d). A door seal is used around the perimeter on the interior of the door (see Figure 5e). When the door is closed and latched, the seal is compressed.

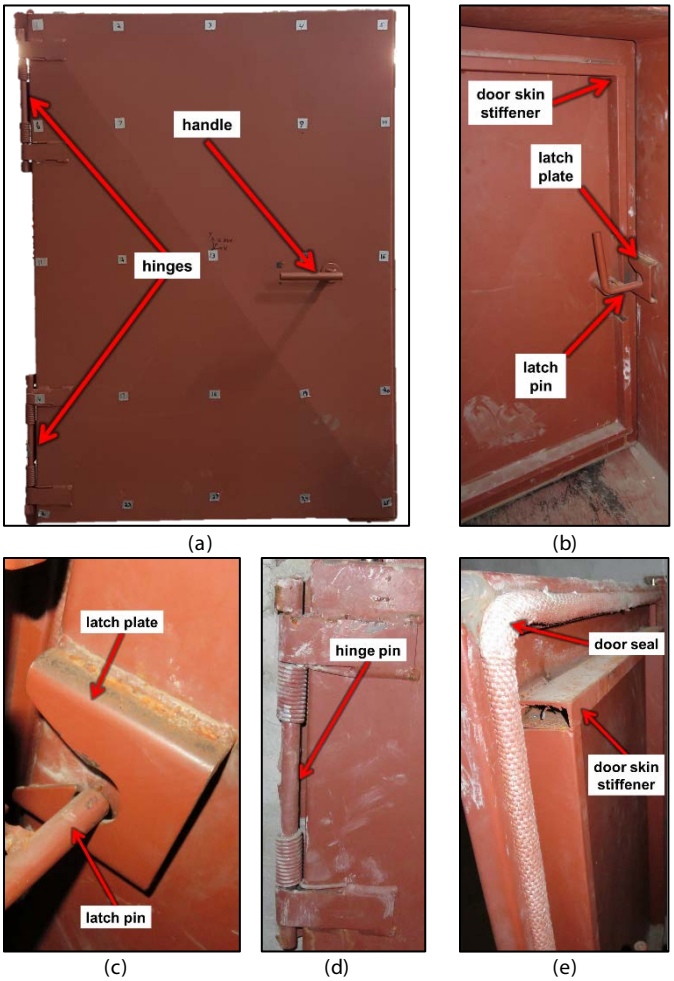

Figure 5. (a) External view of door leaf, (b) internal view of door, (c) close up view of door latch pin and latch plate, (d) close up view of hinge pin, and (e) close up view of door skin stiffener and door seal.

Finite Element Model

ANSYS FEA software was used to create a linear, static model of the door (see Figure 6). The model includes the door skin, door skin stiffener, hinges, handle, latch pin, latch plate, and door seal. The latch pin and latch plate were modeled to be in contact and bonded together. The interfaces between the two hinge pins and their support structure were modeled to be in contact with sliding. The hinge springs were not modeled because they were assumed to have a negligible effect on the loads carried by the door components. The interfaces between components were treated as solid; welded connections between components were not modeled. Therefore, stress concentrations due to weld geometry were not examined by the model.

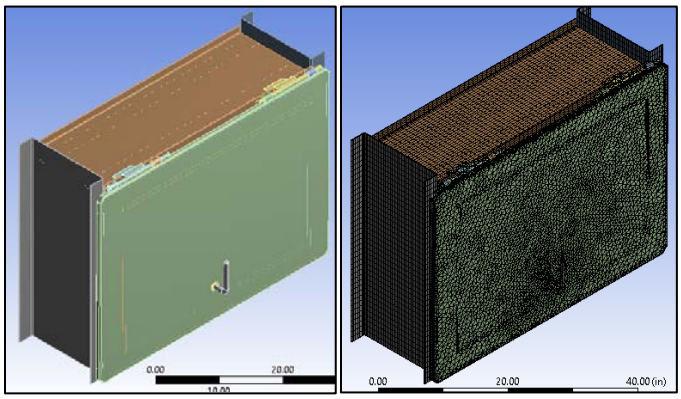

(a) (b)

Figure 6. Finite element model of the door showing (a) solid model and (b) mesh.

Because a BIP RA door should not yield, non-linear material behavior due to yielding was not modeled. The door material was assumed to be ASTM A36 steel with a Young's Modulus of 207 GPa (30,000,000 psi), a Poisson's Ratio of 0.3, and a yield strength of 248 MPa (36,000 psi) [16]. The door seal material was modeled as rubber with a Young's Modulus of 1 MPa (145 psi) and a Poisson's Ratio of 0.5. It is assumed that the material properties of the door seal will have a minimal effect on the stresses imposed on the door components. The load due to compressing the door seal as the door is held closed by the latch is assumed to be about 445 N (100 lb). Considering that a 6.9-kPa (1-psi) load applied to the door skin places a total load of 6,670 N (1,500 lb) on the door, the preload caused by compressing the door seal was ignored. Static and dynamic increase factors were not considered in this analysis.

Different types of elements were used for each of the 28 door components to create the FE mesh. Brick elements were used to mesh the door frame, door skin stiffener, and hinge cylinders. Solid tetrahedral elements [17] were used to mesh the door skin, latch plate, hinge pins, latch pin, and door seal. The final model consisted of 59,463 elements with 281,140 nodes.

Load Conditions

To examine the door response to positive blast pressure loading, the 103.4-kPa (15-psi), 0.2-second-duration design load was used. Next, to examine the door response to negative blast pressure loading, a 20.7-kPa (3-psi), 0.5-second-duration isosceles-triangle-shaped pressure load was assumed based on the pressure traces of Figure 4. It is important to note that this approach completely ignores the internal strain energy that would occur due to the positive loading. The release of this internal strain energy could add to the loads applied to the hinges and latching mechanisms. In addition, the shape of the negative part of the pressure curve resembles a half-sine wave rather than an isosceles triangle. However, assuming that the load is isosceles-triangle-shaped is sufficient for a first-cut analysis. For increased accuracy, a non-linear dynamic analysis would have to be performed so that the actual dynamic load could be applied and both geometric and material non-linear behavior could be modeled.

In order to determine the maximum DLF for the two loads used for the analysis, the approach from *Biggs*, *Chapter 5* [12] was used to determine the effective mass, effective stiffness, and natural period for the door skin. For these calculations, the door skin was assumed to be simply supported around its perimeter. Because the door is not simply supported for negative loading, the effective stiffness of the door for the negative loading will be overestimated, and this will reduce the predicted natural period. In addition, the stiffening effects of the door skin support tube and the x-shaped raised profile on the door skin were ignored. Both of these design features would tend to increase the effective stiffness of the door, which would decrease the natural period of the door. The mass of the door skin support tube was also ignored in the model. Because the effective mass of the door accounts for the parts of the door that experience the most motion during its transient response, and the stiffening tube is around the perimeter of the door where the least motion would occur, the effect of ignoring the mass of the stiffening tube is likely small. The effective mass, stiffness, and natural period of the door were found to be 7.5 kg (0.043 lb-s^2/in), 50.8 kN/m (290 lb/in), and 0.0765 sec, respectively.

The predicted natural period of the door was used to determine the maximum DLF for both the positive and negative load cases. Considering the design load with t_d equal to 0.2 sec, the ratio of the blast load duration to the natural period of the structure is 2.6. From Figure 2, the maximum DLF is about 1.1. For analysis purposes, a DLF value of 1 was used. For the negative pressure load, the duration is 0.5 sec, and the ratio of the load duration to the natural period of the structure is 6.5. Because Figure 2 does not show the maximum DLF for t_d/T ratios above 4.0, it was assumed that the maximum DLF would be 1. Because a value of 1 was used for the maximum DLF for each load, the positive load analysis was carried out with a 103.4-kPa (15-psi) load and the negative load analysis was carried out with a 20.7-kPa (3-psi) load. Each of these loads were applied uniformly to the exterior of the door skin.

RESULTS

103.4-kPa (15-psi) Positive Load

The 103.4-kPa (15-psi) positive load caused yielding of nearly the entire door skin (see Figure 7a). Considering that the yield strength of the assumed material is 248.2 kPa (36,000 psi), almost the entire door skin within the location of the door skin stiffener exceeded the yield strength. The highest stress occurred at the location where the door handle/latch pin goes through the door skin (see Figure 7b). The stress at this location was 4.6 GPa (668,000 psi), almost twenty times the yield strength of the material. In addition, the hinge pins also exceeded the yield strength. The maximum deflection, 122 mm (4.8 in), occurred at the center of the door skin.

The results show that the latch pin and latch plate also exceeded the yield strength (see Figure 7b). The highest stresses on the latch pin occurred near the bend that is close to the door handle-latch pin pass-through. The geometric discontinuity between these parts acts as a stress riser.

20.7-kPa (3-psi) Negative Load

The 20.7-kPa (3-psi) negative load also caused yielding of the door skin in several locations. However, the yielding was localized to the areas where the door handle/latch pin passes through the door and in between the hinge locations (see Figure 8a). The maximum stress on the door skin was 2.2 GPa (315,500 psi), nearly ten times the yield strength. Similar to the 103.4-kPa (15-psi) positive pressure load case, the maximum stress on the door skin was at the interface between the door handle-latch pin pass-through and the door skin. The maximum deflection of the door skin, which occurred at its center, was 25.4 mm (1.0 in).

The latch pin and latch plate also exceeded the yield strength. The maximum stress on the latch plate was 1.6 GPa (236,800 psi), more than six times the yield strength of A36 steel. The latch pin yielded at the 90-degree bend where it exits the door handle-latch pin pass-through. Once again, the geometric discontinuity between these components acts as a stress riser.

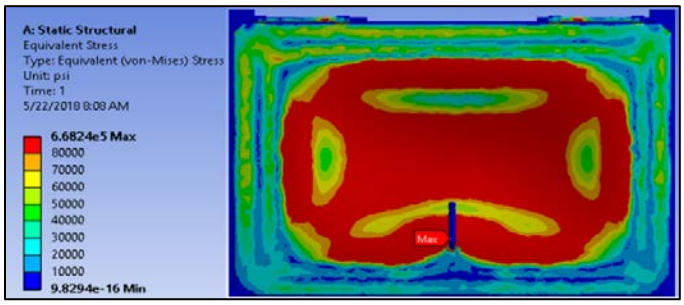

(a)

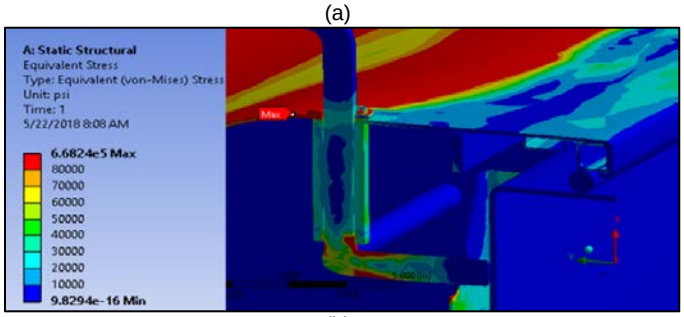

(b)

Figure 7. Von Mises stress distribution resulting from 103.4-kPa (15-psi) positive pressure loading on: (a) door skin and hinges and (b) close-up view of latch pin.

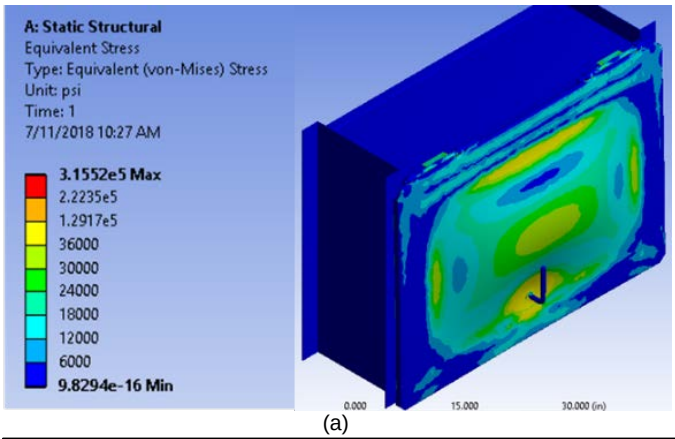

(a)

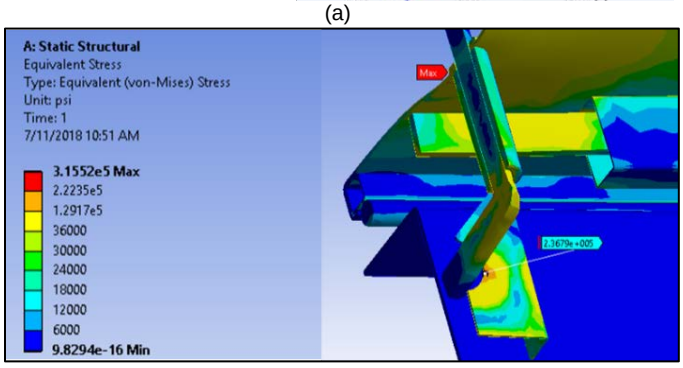

(b)

Figure 8. Von Mises stress distribution resulting from 20.7-kPa (3-psi) negative pressure loading: (a) door skin and hinges and (b) close-up view of latch pin.

DISCUSSION

Assuming a linear elastic response, the blast response of BIP RA doors can be conducted using the maximum DLF approach from *Biggs* [12] to scale the dynamic load applied to the door so that a static analysis can be conducted rather than a dynamic analysis. In this approach, the shape of the blast pressure curve must be considered so that the appropriate DLF curve is used. In addition, the ratio of the blast load duration to the natural period of the door has to be estimated. For increased accuracy, an experimental modal analysis on a door can be used to determine the lowest natural period. Even though the maximum DLF used for both loads was 1 for this specific door design, the maximum DLF may not be 1 for other door designs, depending on the effective mass, effective stiffness, and natural period of the door. The blast duration also impacts the maximum DLF value used.

The door was shown to yield for both the positive 103.4-kPa (15-psi) load case that corresponds to the design load mandated by federal regulations and for the 20.7-kPa (3-psi) negative load case based on Lake Lynn data. It should be noted that the stresses and deflections predicted by the model do not account for non-linear material behavior due to yielding. Furthermore, the model does not include the welds between components. This can also affect the predicted stresses. Therefore, the predicted stresses and deflections could be significantly higher than what would be predicted if material non-linearity due to yielding and weld geometry were modeled. Although several assumptions were made in this analysis, the material yield strength was exceeded by such a wide margin that yielding would occur even if a more detailed analysis was performed.

The door skin, hinges, latch pin, and latch plate were all shown to yield. If these components would yield, the door might not be able to be opened by miners trying to enter an RA. In addition, it is unlikely that the door would seal properly, and contaminated mine air could enter the RA. Therefore, the door design would need to be modified to ensure yielding would not occur. It is important to note that the analysis discussed here did not examine the sealing capability of the door. To analyze the sealing capability of the door, a more accurate model and a non-linear dynamic analysis would be necessary.

To check the validity of the positive-load-case results, a simple analysis was performed to calculate the maximum stress and maximum deflection on the door skin [18]. In this simple analysis, the door skin stiffener and x-shaped raised profile were ignored and fixed boundary conditions were assumed. The actual boundary conditions for the door skin are not easily defined as the door has multiple constraints. In the simple analysis, the full height and width of the door were used, even though the door seal around the perimeter could act as a support. The simplified analysis showed a maximum stress of 4.3 GPa (627,000 psi) compared to 4.6 GPa (668,000 psi) for the FE analysis, and a maximum deflection of 0.30 m (12.0 inches) compared to 0.12 m (4.8 inches) for the FE analysis. It should be noted that the simplified analysis ignores the effect of the door skin stiffener. Because the door skin stiffener reduces the unsupported span of the door skin, the stiffener would have a significant effect on the door skin deflection, so the large disparity between the predictions is not surprising. In addition, the FE model is affected by discontinuities between components. These discontinuities tend to act as stress risers.

In the event of an inescapable accident, BIP RA doors must open easily so that miners can quickly enter the RA and also close and seal properly to prevent contaminated air from entering the RA. To ensure the door would function properly, it must not yield when exposed to the assumed blast loads. To reduce the stresses below the yield strength of the door material, the door's design would have to be modified. Numerous design changes could be made to reduce the stresses on the parts that yielded.

First, the thicknesses of the components could be increased to reduce the stresses. For a rectangular plate loaded in bending, such as the door skin, the maximum stress is inversely proportional to the plate thickness squared [18]. Therefore, doubling the door skin thickness would reduce its maximum stress by a factor of four, tripling its thickness would reduce the maximum stress by a factor of nine, and so on. The door latch pin and hinge pins are similar to beams. For a beam with a round cross section, the maximum bending load is inversely related to the bar diameter cubed [19]. Therefore, doubling the latch-pin or hinge-pin diameters would decrease their stresses by a factor of eight. This is probably not practical, but increasing the pin diameters by even 10% would decrease the bending stresses by 25%.

The latch plate is primarily exposed to shear loading. For shear loading, the stress is proportional to thickness [20]. Thus, doubling the latch plate thickness will reduce its stress by a factor of two.

Because the stresses on the door components are so high, in order to reduce the stresses below the material yield strength, it is likely that the door design would need to be modified in addition to increasing component thicknesses. To reduce the door skin stress, door skin stiffeners could be added to split up the unsupported area of the door skin into smaller areas. For a flat plate, the stress is directly proportional to the square of its span [18]. Therefore, adding a single vertical stiffener located halfway across the width of the door would reduce the stress on the door skin by a factor of four. In addition, this would reduce the deflection of the door skin, which could impact the load carried by the hinge pins, latch pin, and latch plate. The stress along the hinge side of the door skin between the hinges exceeds the material yield strength (refer to Figures 7a and 8a). This load is transferred to the hinge pins. Adding a third hinge could significantly reduce the flexing of the door skin between the hinges, which would in turn reduce the stresses on the hinge pins. Finally, the number of latching locations could be increased.

Assuming that all of the latching locations are along the same door edge, one additional latch would reduce the latch pin and latch plate loads by a factor of two, and two additional latches would reduce the latch pin and latch plate loads by a factor of three.

CONCLUSIONS

BIP RA doors must be able to withstand survivable mine explosions without yielding so that the doors can be opened and can maintain a good seal. When analyzing BIP RA doors, both positive and negative pressure loads must be considered. In order to use a static analysis to examine the door's dynamic response, the maximum DLF approach can be used to scale the static load by the appropriate factor based on the door's natural period, the blast shape, and the blast duration. For doors with simple components, closed-form solutions can be used to estimate the resulting stress and displacement. For more complex cases, linear static FE analysis can be used with the maximum-DLF-scaled positive and negative pressure loads. In spite of the negative pressure being much lower than the peak positive pressure, negative pressure effects must be examined.

For the loads used here, yielding was predicted at numerous locations, including the door skin, the hinges, the latch pin, and the latch plate. In order to ensure the door would survive the blast loads without yielding, component thicknesses would need to be increased and/or the door design would need to be modified.

LIMITATIONS

The door analysis presented here examines only one blast from Lake Lynn data. Additional blast data should be reviewed to examine the shapes and amplitudes of a wide range of blasts to determine an appropriate set of design pressure magnitudes, shapes, and durations that can be applied to BIP RA door designs. The FE model makes several simplifications and has not yet been benchmarked against test data. However, because the predicted loads were much higher than the door material yield strength, the model seems adequate for a first-cut analysis. The suggested design changes are based on engineering design principles, but these changes should be verified by additional modeling and/or testing.

DISCLAIMER

The findings and conclusions in this paper are those of the authors and do not necessarily represent the official position of the National Institute for Occupational Safety and Health, Centers for Disease Control and Prevention. Mention of any company or product does not constitute endorsement by NIOSH.

REFERENCES

Federal Register, 2008, "Refuge Alternatives for Underground Coal Mines; Final Rule," Department of Labor, Mine Safety and Health Administration, 30 CFR Parts 7 and 75, Wednesday, December 31, pp. 80656-80700. http://www.msha.gov/REGS/FEDREG/FINAL/2008finl/E8-30669.pdf

1. "Historical Data on Mine Disasters in the United States" MSHA, accessed 9/14/2018. https://arlweb.msha.gov/mshainfo/factsheets/mshafct8.htm.
2. Ounanian, D., 2008, "Refuge Alternatives in Underground Coal Mines", FMI Report No: NSH-080020-1864, Final Report – Volume I, Contract Number: 200-2007-20276, December 2008. https://www.cdc.gov/niosh/mining/researchprogram/contracts/contract_200-2007-20276.html.
3. MSHA, 2006, "REPORT OF INVESTIGATION: Fatal Underground Coal Mine Explosion January 2, 2006 Sago Mine, Wolf Run Mining Company Tallmansville, Upshur County, West Virginia ID No. 46-08791", United States Department of Labor, Mine Safety and Health Administration, Coal Mine Safety and Health. https://arlweb.msha.gov/Fatals/2006/Sago/ftl06C1-12wa.pdf.
4. Zipf, R.K., Cashdollar, K.L., "Effects of blast pressure on structures and the human body", NIOSH accessed 9/14/2018. https://www.cdc.gov/niosh/docket/archive/pdfs/NIOSH-125/125-ExplosionsandRefugeChambers.pdf
5. Glasstone S., Dolan P.J., eds., 1977, The effects of nuclear weapons. 3rd ed. U.S. Department of Defense and the Energy Research and Development Administration.
6. Sartori, L., 1983, The effects of nuclear weapons, Physics Today, March, pp. 32-41.
7. ARMY Manual TM 5-1300, 1990, Department of the Army, Washington, DC.
8. MSHA, 2013, "QUESTIONS AND ANSWERS MSHA'S REFUGE ALTERNATIVES REQUIREMENTS, https://arlweb.msha.gov/REGS/COMPLIAN/GUIDES/RefugeAlternatives.pdf.
9. Zipf, K., Weiss, E.S., Harteis, S.P., and Sapko, M.J., 2009, "Compendium of Structural Testing Data for 20-psi Coal Mine Seals," U.S. Department of Health and Human Services, Centers for Disease Control and Prevention, National Institute for Occupational Safety and Health, Pittsburgh, PA, Information Circular, IC 9515, 143 pp. https://www.cdc.gov/niosh/mining/works/coversheet710.html.
10. Trackemas, J.D., Thimons, E.D., Bauer, E.R., Sapko, M.J., Zipf, R.K., Schall, J., Rubinstein, E., Finfinger, G.L., Patts, L.D., and LaBranche, N., 2015, "Facilitating the Use of Built-in-place Refuge Alternatives in Mines," U.S. Department of Health and Human Services, Centers for Disease Control and Prevention, National Institute for Occupational Safety and Health, Pittsburgh, PA, Report of Investigations, RI 9698, 80 pp.
11. Biggs, J.M., 1964, "Introduction to Structural Dynamics", McGraw-Hill, New York.
12. Avallone, E.A., Baumeister III, T., Sadegh, A.M., 2007, "Marks' Standard Handbook for Mechanical Engineers 11th Edition", McGraw-Hill, New York.
13. Young, W.C., Budynas, R.G., Sadegh, A.M., 2012, "Roark's Formulas for Stress and Strain, 8th Edition", McGraw-Hill, New York.
14. Sapko, M.J., Weiss, E.S., Trackemas, J., and Stephan, C.R., 2004, "Designs for rapid in situ sealing", Trans Soc Min Metall Explor 2004 Jan; 316:85-92. https://www.cdc.gov/niosh/mining/works/coversheet1087.html.
15. MatWeb, 2018, Material Property Data for ASTM A36 Steel, bar, accessed 9-24-2018. http://www.matweb.com/search/datasheet_print.aspx?matguid=d1844977c5c8440cb9a3a967f8909c3a.

16. Wang, E., Nelson, T., and Rauch, R., 2004, “Back to Elements - Tetrahedra vs. Hexahedra” 2004 International ANSYS Conference. https://support.ansys.com/staticassets/ANSYS/staticassets/resourcelibrary/confpaper/2004-Int-ANSYS-Conf-9.PDF.

17. Roymechx, 2018, Rectangular Plates, accessed 9-24-2018. http://www.roymech.co.uk/Useful_Tables/Mechanics/Plates.html

18. MechaniCalc, 2018, Stresses & Deflections in Beams: Bending Stresses in Beams, accessed 9-24-2018. https://mechanicalc.com/reference/beam-analysis#bending-stress-in-beam.

19. Engineers Edge, 2018, Shear Stress Equations and Applications, accessed 9-24-2018. https://www.engineersedge.com/material_science/shear-stress.htm.